JOURNAL OF CATALYSIS **169,** 132–142 (1997)
ARTICLE NO. CA971680

FTIR Spectroscopic Study and CO Hydrogenation on V, Nb, and Ta Oxide Promoted Rh/SiO_2 Catalysts

T. Beutel,*[,1] O. S. Alekseev,† Yu. A. Ryndin,† V. A. Likholobov,† and H. Knözinger*

*Institut für Physikalische Chemie, Universität München, Sophienstr. 11, 80333 Munich, Germany; and †Boreskov Institute of Catalysis, Prospekt Akademika Lavrentieva 5, Novosibirsk 690090, Russia

Received October 28, 1996; revised February 12, 1997; accepted February 12, 1997

The CO hydrogenation over Rh/SiO_2 catalysts promoted with oxides of Vb transition metals was studied. Two different kinds of promoter effects occurred which were established by high temperature reduction (HT reduction, $T_{red} \geq 673$ K) and HT calcination ($T_{calc} \geq 973$ K), followed by reduction at 673 K, respectively. While HT reduction favors formation of ethanol, HT calcination, followed by reduction at 673 K enhances the selectivity toward methanol. The overall activity increased in the order V < Nb < Ta. The impact of promotion on the metal state was characterized by FTIR spectroscopy of adsorbed CO at 85 K. Modification of Rh/SiO_2 with promoter oxide causes a slight high frequency shift for linearly bonded CO on rhodium. Reduction at 673 K leads to a decrease in CO chemisorption capacity. In this state the rhodium metal surface is thought to be partially covered by promoter oxide and hence compares to the conventional SMSI state. This effect is enhanced if the reduction is preceded by HT calcination. The capability of the promoter oxide to spread over the metal surface increases in the order Ta < Nb < V. While the total CO chemisorption capacity is lowered in the SMSI state, the relative amount of linearly to bridge-bonded CO increases and characteristic changes in the band shape of bridge-bonded CO occur. A high frequency component at around 1920 cm^{-1} characteristic of bridge-bonded CO which is present after LT reduction ($T_{red} = 573$ K) disappears after HT reduction.

INTRODUCTION

Silica supported, promoted rhodium catalysts are extensively studied in the CO hydrogenation reaction because they exhibit an exceptionally high selectivity towards oxygenated products (1–13). As promoter materials Vb transition metal oxides have found special attention, in particular V oxide (14–28). Less widely studied are Nb oxide (29–33) and Ta oxide (34) promoted rhodium catalysts. This work presents the first comparative study of the promoting properties of V, Nb, and Ta oxides on the CO hydrogenation over Rh/SiO_2.

[1] Present address: Laboratoire de Réactivité de Surface, 1106 URA du CNRS, Université P. et M. Curie, 4 Place Jussieu, 75252 Paris Cedex 05, France.

Many factors have been shown to be critical for the activity and selectivity of these catalysts. These can be devided in reaction conditions and catalyst related properties, such as preparation methods, and catalyst composition. The present study focuses on sample specific parameters, namely the influence of the nature of the promoter element choosing Vb transition metal oxides as well as temperature effects induced by pretreatments in air (T_{calc}) and hydrogen (T_{red}).

The influence of the temperature of reduction has been extensively investigated and one important phenomenon arose: The SMSI (strong metal support interaction) effect. This term was coined by Tauster and Fung (35) who found in 1978 that high temperature reduction of transition metal oxide promoted noble metal catalysts provoked a dramatic decrease in CO and H_2 chemisorption capacities. The metal dispersion in M°/XO_y systems (M = noble metal, XO_y = promoter oxide) is high in the SMSI state. Several theories have been discussed including formation of MX_y alloys (36), electronic effects of the promoter oxide such as polarization of small metal clusters (37) or electron transfer via direct bond formation between cus promoter sites and metal atoms (38), and a mere physical blocking of metal particles by promoter oxide (19, 39–42). Among these explanations of the SMSI effect, the last one is most favored in recent literature, although the action of additional electronic effects is by no means excluded. The conventional SMSI effect, induced by HT reduction and its impact on the catalytic properties of promoted Rh/SiO_2 catalysts is well studied (14–18, 21–24, 43).

Another type of metal promoter oxide interactions can be achieved by HT calcination and has been described previously for Rh/SiO_2 catalysts promoted by Vb transition metal oxides (44–49). It has been demonstrated earlier that mixed oxides, $RhXO_4$ (X = V, Nb, Ta), are formed at $T_{calc} \geq 973$ K. Subsequent reduction of these mixed oxides results in well-dispersed Rh° metal particles occluded in promoter oxide. While the formation, reduction, and catalytic behavior of $RhVO_4$ and $RhNbO_4$ are well studied, there is to our knowledge no study on supported $RhTaO_4$.

0021-9517/97 $25.00

Another subject of this work is, therefore, to study the influence of the temperature of calcination on the catalytic properties of $Rh/X/SiO_2$ (X = V, Nb, Ta) catalysts.

In this work we use FTIR spectroscopy with CO as a probe molecule to elaborate metal dispersions and metal promoter oxide interactions, which are induced by either HT reduction or HT calcination.

EXPERIMENTAL

Sample Preparation

Promoted Rh/SiO_2 catalysts were prepared by stepwise impregnation of precalcined silica (Alpha Products, 330 m^2/g, $T_{calc} = 773$ K) with an aqueous solution of NH_4VO_3 (Fluka, >99%) + oxalic acid (Merck, >99%), niobic acid ($Nb_2O_5 \times H_2O$, CBMM, AD/620) + oxalic acid, or a commercial tantalum oxalate solution (HCST, 145 g Ta_2O_5/l), respectively. In the first impregnation step a suspension of 10 g SiO_2 was unified with the oxalic acid solution of the respective Vb transition metal. The total volume of the suspension was 200 ml in the case of V- and Ta-containing catalysts, the ratio $H_2C_2O_4$: V being 4 in the case of V-containing catalysts. The poor solubility of $Nb_2O_5 \times H_2O$ required to increase the amount of oxalic acid corresponding to a ratio of $H_2C_2O_4$: Nb = 23. The total volume of the suspension was 400 ml for Nb-containing catalysts.

The suspensions were stirred for 1 h at room temperature (r.t.) prior to evaporation of the solvent at a pressure of 25 mbar and T = 333 K. Samples were then dried in air at 383 K for 12 h, ground in an agate mortar and calcined at 773 K for 3 h in order to decompose Vb-metal oxalate complexes. These materials were subsequently impregnated with an aqueous solution of $Rh(NO_3)_3$. Removal of water and subsequent drying were performed as after the first impregnation step. The samples were then submitted to a 7 h calcination at 573, 773, 973, and 1173 K, respectively. The resulting catalysts are denoted as Rh/X/573, Rh/X/773, Rh/X/973, and Rh/X/1173 with X = V, Nb, Ta. The nominal Rh loading was 3 wt%, the ratio X : Rh = 4 for all promoted Rh/SiO_2 catalysts. All calcinations were carried out in a Muffle-furnace in air at a heating rate of 5 K/min.

As reference substances, unpromoted Rh/SiO_2 catalysts were prepared following the recipe described above. These samples are accordingly denoted Rh/573, Rh/773, Rh/973, and Rh/1173, and contain 3 wt% Rh.

Experimental Methods

FTIR spectroscopy. For FTIR spectroscopy, samples were pressed at 10^2 bar into self-supporting wafers of 10–15 mg weight per cm^2. Spectra were recorded in transmission on a Bruker IFS66 FTIR spectrometer at a resolution of 2 cm^{-1}; 64 scans were accumulated using an MCT detector. Spectra are corrected for background absorbance and the sample mass exposed to the beam (see below). Wafers were placed in a copper cell, described earlier (50), which had CaF_2 windows and could be evacuated to 10^{-5} mbar. Catalysts were pretreated in situ in O_2 (Linde 4.5) at 573 K in order to clean the surface from hydrocarbon contaminations. Subsequent reduction was performed in a flow of H_2 (Linde 5.0) at a flow rate of 50 ml/min and a heating ramp of 5 K/min starting at 333 K. H_2 treatments were carried out at 523 K (low temperature reduction), 673 K and 773 K (high temperature reduction) for 2 h. After evacuation of the samples for 1 h at the respective temperature of reduction, catalysts were cooled to 85 K and exposed to CO.

CO hydrogenation. Co hydrogenation reactions were carried out in a flow differential reactor at 523 K, a total pressure of 10 bar and an H_2 : CO ratio of 2. The space velocity was 20000 h^{-1} and the overall conversion was kept below 5%. The reaction products (C_1–C_4 hydrocarbons, acetaldehyde, methanol, and ethanol) were separated chromatographically using a Porapak R column and detected by FID (flame ionization detector). Prior to activity measurements, catalysts were reduced in situ in H_2 at 523, 673, or 773 K.

Activity is expressed as A_i = mmol CO/molRh $*$ s, where the numerator denotes the amount of CO converted into product *i*. The total activiy is defined as $A_{tot} = \sum A_i$. In order to calculate turnover frequencies (TOF), total activities were normalized by CO chemisorption capacities measured at room temperature as reported elsewhere (51). The turn-over frequency is defined as $TOF = A_{tot}/D\ 10^{-3}$ [s^{-1}]. $D = Rh_s/Rh_{tot}$, where Rh_s was equalized with the amount of chemisorbed CO and Rh_{tot} is the total amount of Rh in the sample. Note that the dispersion D cannot be correlated with the metal particle size for promoted Rh/SiO_2 catalysts because of partial encapsulation of the metal by promoter oxide. Selectivity is expressed as carbon efficiency, $S_i = A_i/\sum A_i$, and defined as the amount of CO converted into product *i* relative to the total amount of converted CO.

RESULTS

FTIR spectroscopy. Figures 1A and B show the carbonyl spectra of unpromoted and promoted Rh/SiO_2 catalysts after calcination at 573 K and subsequent reduction at 673 K. In Fig. 1A, samples were exposed to 100 mbar CO at 85 K and then evacuated. The dominating features are linearly and bridge-bonded CO with bands at 2069 and 1898 cm^{-1}, respectively, for Rh/573 (52, 53). It is obvious that the CO chemisorption capacity decreases in the order Rh/573 ≈ Rh/Ta/573 > Rh/Nb/573 > Rh/V/573. This is in line with CO chemisorption measurements that have been carried out separately under flow conditions as reported elsewhere (51). The band shape of bridge-bonded CO on Rh° in spectrum a of Fig. 1A suggests the presence

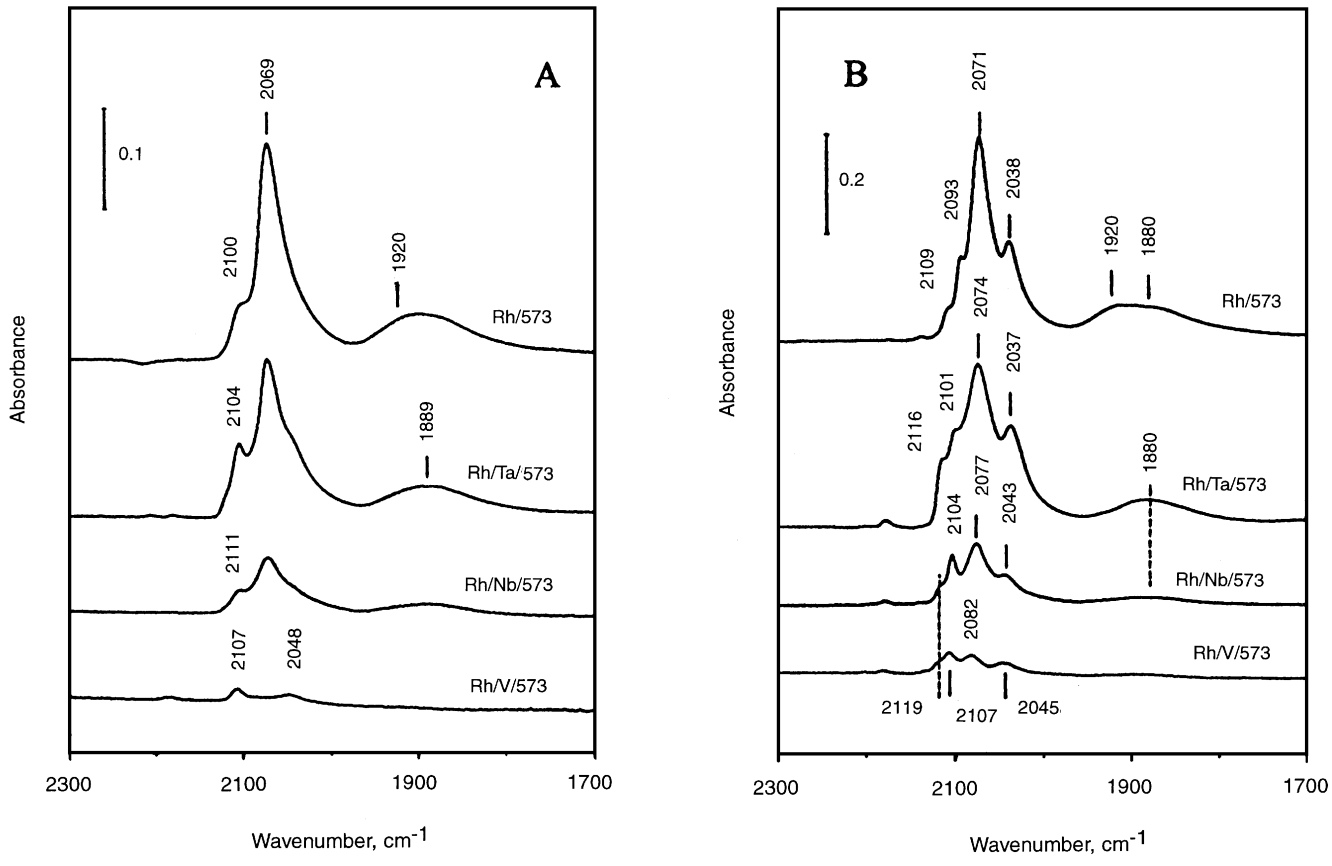

FIG. 1. FTIR spectra in the ν_{CO} region of Rh/SiO_2, $Rh/Ta/SiO_2$, $Rh/Nb/SiO_2$, and $Rh/V/SiO_2$ calcined at 573 K and subsequently reduced at 673 K, after exposure to 100 mbar CO at 85 K and subsequent 5 min evacuation (A), and after warming in 100 mbar CO to 290 K (B).

of two components at around 1920 and 1890 cm^{-1}. Interestingly, the band structure of bridging CO ligands changes upon promotion. The broad contribution at 1920 cm^{-1} in Rh/573 is depleted or eroded in promoted catalysts (spectra b, c, and d in Fig. 1A). $Rh/X/SiO_2$ samples show mainly a single broad absorption band around 1890 cm^{-1} in the region of bridging CO; CO bonded to metallic Rh° dominates in Nb and Ta promoted Rh/SiO_2 catalysts, but is not observed for Rh/V/573. In the latter sample, terminal and bridge-bonded CO on Rh° is absent and only weak bands at 2107 and 2048 cm^{-1} are observed which are attributed to $Rh^+(CO)_2$ cations (54, 55). Figure 1B shows the spectra after warming up to room temperature in 100 mbar CO. While features typical for Rh° bonded CO are essentially unaltered, twin band intensities clearly increase in all samples. There is a blue shift of the center of twin bands measured at room temperature in promoted Rh/X/573 catalysts with decreasing atomic number of the promoter element as shown in Fig. 6 below.

Figures 2A and B show the effect of reduction temperature on the LT adsorption of CO on Rh/Nb/573 and Rh/Ta/573, respectively. It is apparent that the overall band intensity decreases with increasing temperature of reduction. Interesting changes occur in the region of bridge-bonded CO. After LT reduction, there is a contribution at about 1920 cm^{-1} which is gradually extinguished as reduction temperatures are raised.

In order to further analyze the spectra, bands characteristic of the three adsorption states of CO, namely $Rh^+(CO)_2$ cations, linearly and bridge-bonded CO on Rh° were decomposed and their integrated intensities were measured. The spectral part of the linear absorption band was determined by subtracting the integral intensity of the twin bands. The contribution of the latter was evaluated by a fit of the better resolved band of the symmetric CO stretching frequency using a Gaussian function and a fwhh of 15 to 20 cm^{-1}. Assuming an OC–Rh–CO bond angle of 90°, the corresponding antisymmetric stretching frequency should have equal intensity (56). The separation of linearly from bridge-bonded CO was carried out at the local minimum of the corresponding bands. In order to correct deviations of the wafer thickness of different samples, signal intensities were normalized to the amount of sample exposed in the IR beam using the integral intensity of combination and overtone bands of the SiO_2 support. Support bands were integrated in the range between 1550 and 2150 cm^{-1}. The

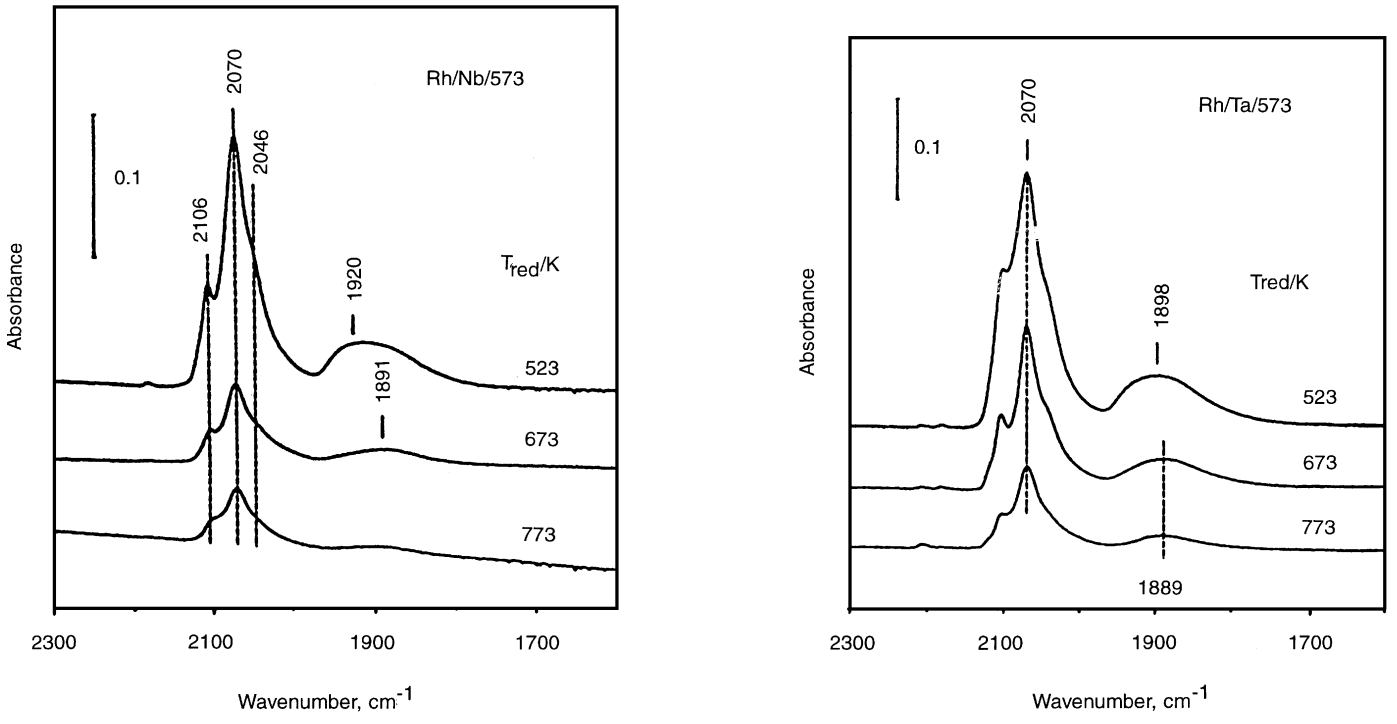

FIG. 2. FTIR spectra in the ν_{CO} region of $Rh/Nb/SiO_2$ and $Rh/Ta/SiO_2$, calcined at 573 K and subsequently reduced at 523 K (a), 673 K (b), and 773 K (c), followed by exposure to 100 mbar CO at 85 K and subsequent evacuation for 5 min at 85 K.

number of CO oscillators relative to the amount of support is given in Eq. [1]:

$$C_{CO,j} = \frac{n_j}{n_T \times \varepsilon_{I,T}} = \frac{E_{I,j}}{\varepsilon_{I,j} \times E_{I,T}}, \qquad [1]$$

where n_j means the number of CO molecules in adsorption state j and n_T is the number of SiO_4 tetrahedra exposed to the IR beam. $\varepsilon_{I,j}$ and $\varepsilon_{I,T}$ are the integrated extinction coefficients of molecule CO_j and of SiO_4 tetrahedra, respectively, while $E_{I,j}$ and $E_{I,T}$ denote their integrated absorbances. The ratio on the left-hand side of Eq. [1] is a measure of the concentration $C_{CO,j}$, corresponding to the reciprocal ε, of CO oscillators in the sample. Values for $C_{CO,j}$ were calculated measuring $E_{I,j}$ and $E_{I,T}$. Integral extinction coefficients for CO_j were taken from an earlier work by Rasband and Hecker (57):

$$\text{linearly bonded CO, } l: \ \varepsilon_{I,l} = 13 \times 10^6 \text{ cm/mol}$$
$$\text{bridge-bonded CO, } b: \ \varepsilon_{I,b} = 42 \times 10^6 \text{ cm/mol}$$
$$\text{gem dicarbonyl CO, } g: \ \varepsilon_{I,g} = 65 \times 10^6 \text{ cm/mol}.$$

In order to estimate the number of surface Rh° atoms and Rh^+ ions, $C_{CO,j}$ values calculated from Eq. [1] were divided by a stoichiometric factor $z(j)$ with $z(g) = 2$, $z(l) = 1$, and $z(b) = 0.5$. The resulting quantities are specified as $C_{Rh,j}$ having again the dimension of reciprocal ε.

The total concentration of surface rhodium sites is given by Eq. [2]:

$$C_{Rh,tot} = \sum_j C_{Rh,j} = \sum_j \frac{E_{I,j}}{\varepsilon_{I,j} \times E_{I,T} \times z(j)}. \qquad [2]$$

$C_{Rh,tot}$ and l/b ratios were determined after reduction and LT adsorption of CO.

Table 1 compiles IR band positions and intensities of the carbonyl spectra presented in Figs. 1A and B. There is a hypsochromic shift of the frequencies for linearly bonded CO and gem dicarbonyl groups in the order Ta < Nb < V. The concentration of surface Rh atoms decreases in the same order.

With the aim to derive information about the metal particle size or SMSI effects (see below), the ratio of concentrations of linearly and bridge-bonded CO, henceforth referred to as l/b ratio, was evaluated. The l/b ratio is defined as

$$\frac{l}{b} = \frac{C_{CO,l}}{C_{CO,b}}. \qquad [3]$$

Interestingly, there is an increase in l/b ratios upon promotion of Rh/573 with either Nb or Ta oxide (see Table 1).

Table 2 presents the sum of concentrations, $\sum C_{Rh,j} = C_{Rh,tot}$, and l/b ratios of Rh/Nb/573 and Rh/Ta/573 dependent on the reduction temperature. The CO uptake declines

TABLE 1

IR Band Positions and Relative Intensities of CO Adsorbed on Unpromoted and Promoted Rh/SiO_2 Catalysts after Calcination at 573 K Followed by Reduction at 673 K

	Rh/573	Rh/Ta/573	Rh/Nb/573	Rh/V/573
ν_l [cm^{-1}][a]	2071	2074	2077	2082
ν_b [cm^{-1}][a]	1920/1880	1880	1890	1890
ν_g [cm^{-1}][a]	2093/2038	2101/2037	2104/2043	2107/2045
$C_{Rh,tot}$ [b] [10^{-9} mol/cm]	39.6	32.2	8.6	<1
l/b[b]	4.3	7.1	6.6	—

Note. ν_l, ν_b, ν_g denote carbonyl stretching frequencies of linear, bridge-bonded and geminal CO ligands, respectively. $C_{Rh,tot}$ is the total concentration of surface Rh atoms $C_{Rh,tot}$ and l/b the ratio of linearly to bridge-bonded CO as defined in Eqs. [2] and [3], respectively.

[a] Measured in 100 mbar CO at 290 K.

[b] Measured after adsorption of 100 mbar CO at 85 K and subsequent evacuation for 5 min.

with rising temperature of reduction. This behavior is typical for SMSI systems and has been reported earlier for Nb promoted Rh/SiO_2 catalysts (31, 58). Remarkably, there is a dramatic increase in the l/b ratios for both catalysts when the temperature of reduction is increased from 673 to 773 K.

The influence of the calcination temperature on the IR spectra of chemisorbed CO was also studied. Among the systems under investigation, $Rh/Ta/SiO_2$ and the unpromoted reference system Rh/SiO_2 were chosen since promotion with V or Nb oxides is found to eliminate CO uptakes almost completely if the calcination is performed at 973 and 1173 K. Table 3 compares l/b ratios and overall CO chemisorption capacities for $Rh/Ta/SiO_2$ and Rh/SiO_2.

There is a significant decrease in CO uptake with rising calcination temperature for both systems. However, the l/b ratios are almost constant in Rh/SiO_2 and remain lower than in Rh/Ta/573, Rh/Ta/773, and Rh/Ta/973. The l/b ratio decreases in $Rh/Ta/SiO_2$ only after calcination at 1173 K and has the same value as in Rh/1173.

In order to check the influence of promoter oxides on the acidity of the silica support, the band shift of the SiO−H bond was measured by adsorption of CO at 85 K. Figure 3 shows that the position of the H-bonded silanol group is

TABLE 2

Total Concentration of Surface Rh Atoms, $C_{Rh,tot}$, and Ratio of Linearly to Bridge-Bonded CO, l/b, as Defined in Eqs. [2] and [3], Measured for $Rh/Nb/SiO_2$ and $Rh/Ta/SiO_2$ after Calcination at 573 K and Subsequent Reduction at Different Temperatures

Reduction temperature [K]	Rh/Nb/573		Rh/Ta/573	
	$C_{Rh,tot}$ [10^{-9} mol/cm]	l/b	$C_{Rh,tot}$ [10^{-9} mol/cm]	l/b
523	26.4	6.1	45.9	5.5
673	8.6	6.8	32.2	7.1
773	5.7	15.6	14.5	10.9

TABLE 3

Total Concentration of Surface Rh Atoms, $C_{Rh,tot}$, and the Ratio of Linearly to Bridge-Bonded CO, l/b, as Defined in Eqs. [2] and [3], Measured for Rh/SiO_2 and $Rh/Ta/SiO_2$, after Calcination at Different Temperatures, Followed by Reduction at 673 K

Calcination temperature [K]	Rh/SiO_2		$Rh/Ta/SiO_2$	
	$C_{Rh,tot}$ [10^{-9} mol/cm]	l/b	$C_{Rh,tot}$ [10^{-9} mol/cm]	l/b
573	39.6	4.3	32.2	7.1
773	29.9	4.1	24.9	7.3
973	2.8	5.4	6.6	6.0
1173	1.8	3.9	1.1	3.6

constant for unpromoted Rh/573 and promoted Rh/X/573 catalysts, suggesting that there is no impact of the promotion on the acidity of the support material after LT calcination.

CO hydrogenation. Table 4 lists the total activities and selectivities in the CO hydrogenation reaction for Rh/573 after reduction at 523, 673, and 773 K. Methane

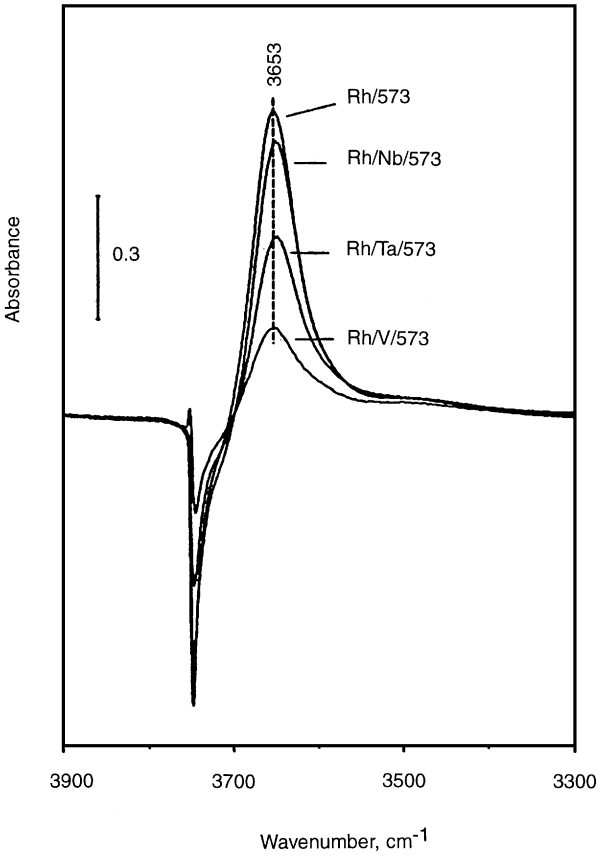

FIG. 3. FTIR difference spectra of the ν_{OH} region of Rh/SiO_2, $Rh/Nb/SiO_2$, $Rh/Ta/SiO_2$, and $Rh/V/SiO_2$, calcined at 573 K and reduced at 673 K prior to adsorption of 50 mbar CO at 85 K. Background spectra before CO adsorption were subtracted.

TABLE 4

Catalytic Properties in CO Hydrogenation after 6 h Time on Stream of Unpromoted Rh Catalysts Calcined at 573 K and Reduced at Different Temperatures

Reduction temperature [K]	Selectivity					Total activity[a]	Turn-over frequency[b]
	C_1[c]	C_{2-4}[d]	AcH[e]	MeOH[f]	EtOH[g]		
523	52.5	15.3	18.8	12.0	1.0	16.4	0.03
673	54.0	10.0	20.8	14.4	0.9	20.7	—
773	57.4	13.0	17.0	11.2	0.9	15.2	0.03

[a] Total activity: A_{tot} = mmol CO/mol Rh × s, 10^{-3} [s^{-1}].
[b] Turn-over frequency: TOF = A_{tot}/D, 10^{-3} [s^{-1}]; D = Rh_s/Rh_{tot}; Rh_s: number of surface rhodium atoms, determined by CO chemisorption, Rh_{tot} = Total amount of rhodium atoms.
[c] Methane.
[d] C_{2-4} hydrocarbons.
[e] Acetaldehyde.
[f] Methanol.
[g] Ethanol.

and acetaldehyde are the main products. Small amounts of methanol are detected, but only traces of ethanol are formed. Total activity and product distribution are essentially independent of the reduction temperature.

Figure 4 shows the total activity of promoted Rh/SiO_2 catalysts after HT reduction as a function of the calcination temperature. Between 573 and 973 K, promotion leads to an increase in total activity as compared to Rh/SiO_2, the extent of which increases with the atomic weight of the promoter element. After calcination at 1173 K, all $Rh/X/SiO_2$ catalysts display about the same total activity which is close to that of unpromoted Rh/573 (see Table 4).

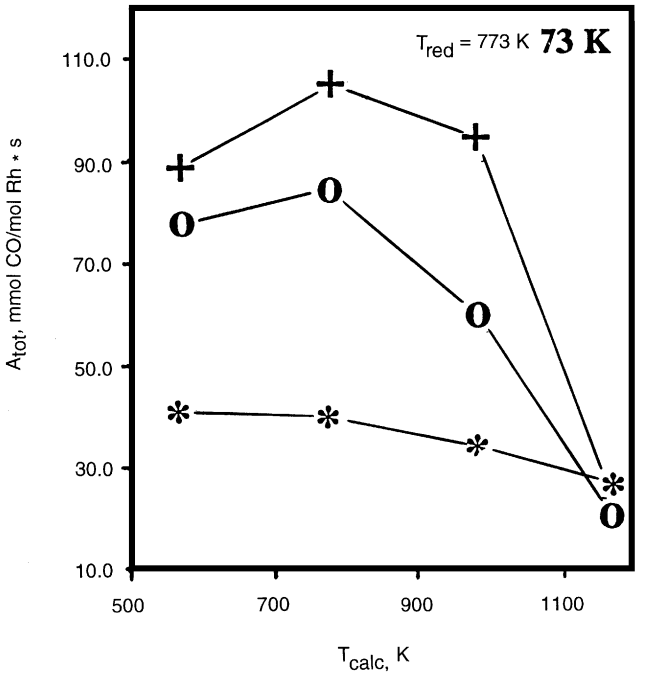

FIG. 4. Effect of calcination temperature on the total activity in CO hydrogenation over $Rh/V/SiO_2$ (∗), $Rh/Nb/SiO_2$ (○), and $Rh/Ta/SiO_2$ (+). Catalysts were reduced at 773 K.

Table 5 compares the catalytic properties of promoted Rh/SiO_2 catalysts after calcination at 573 K and subsequent

TABLE 5

Catalytic Properties in CO Hydrogenation after 6 h Time on Stream of Promoted Rh Catalysts Calcined at 573 K and Reduced at Different Temperatures

Sample	T_{red} [K]	Selectivity					Total activity[a]	Turn-over frequency[b]
		C_1[c]	C_{2-4}[d]	AcH[e]	MeOH[f]	EtOH[g]		
Rh/V/573	523	11.9	7.9	3.3	32.4	44.6	87.9	0.55
	673	13.4	11.8	1.6	32.4	41.0	52.2	0.37
	773	11.1	9.6	0.7	33.5	45.2	40.9	0.58
Rh/Nb/573	523	29.4	13.5	7.3	16.8	33.1	170.4	0.21
	673	18.7	11.3	3.4	18.9	47.4	138.0	0.46
	773	25.7	24.6	3.5	12.2	34.0	78.1	0.41
Rh/Ta/573	523	14.1	5.4	2.9	44.7	33.0	95.2	0.12
	673	21.5	6.1	1.8	28.1	42.6	127.7	0.20
	773	13.7	4.8	1.5	30.5	49.6	87.9	0.20

[a] Total activity: A_{tot} = mmol CO/mol Rh × s, 10^{-3} [s^{-1}].
[b] Turn-over frequency: TOF = A_{tot}/D, 10^{-3} [s^{-1}]; D = Rh_s/Rh_{tot}; Rh_s: number of surface rhodium atoms, determined by CO chemisorption, Rh_{tot} = Total amount of rhodium atoms.
[c] Methane.
[d] C_{2-4} hydrocarbons.
[e] Acetaldehyde.
[f] Methanol.
[g] Ethanol.

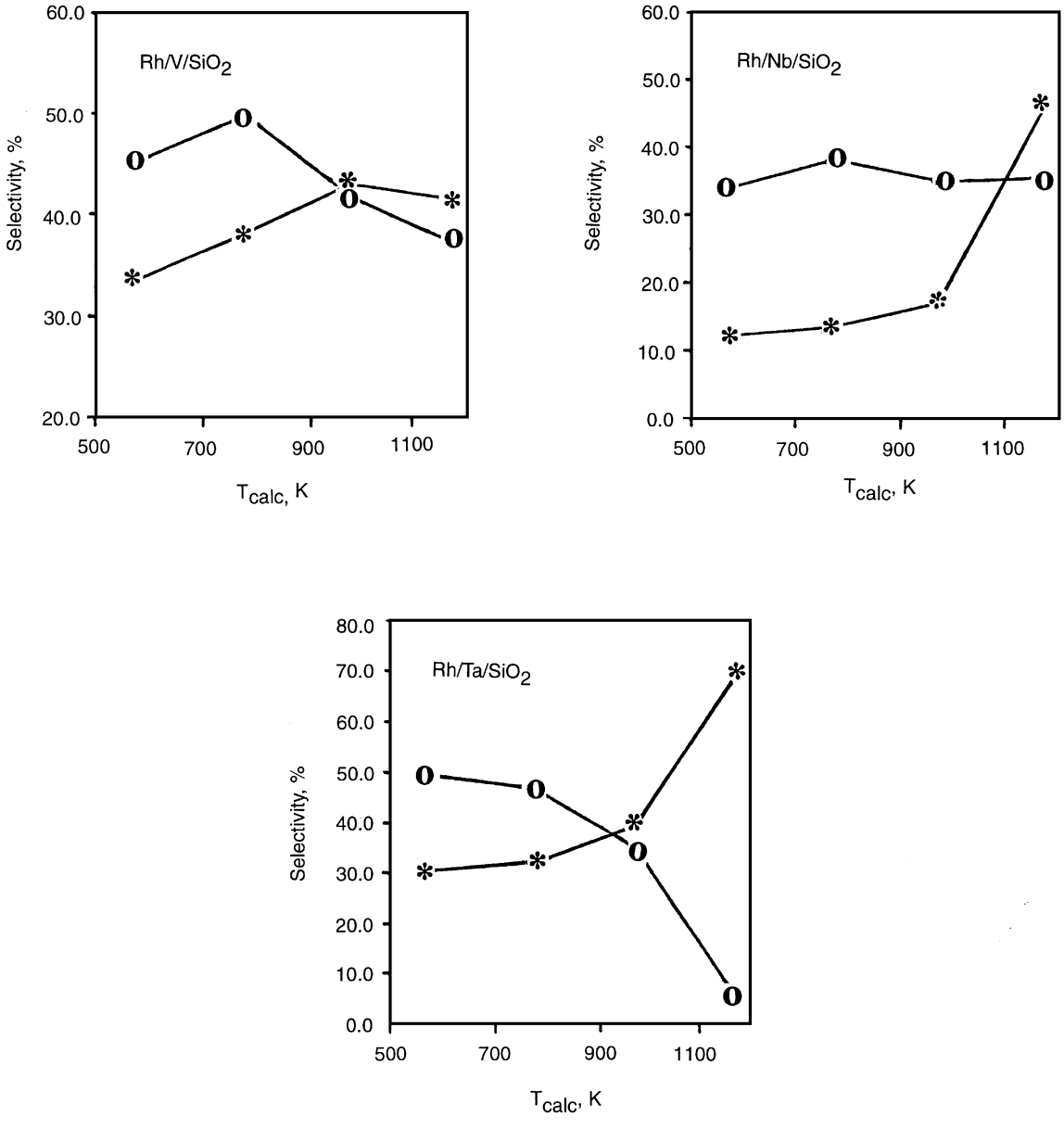

FIG. 5. Effect of calcination temperature on the selectivity toward methanol (∗) and ethanol (○) of $Rh/V/SiO_2$, $Rh/Nb/SiO_2$, and $Rh/Ta/SiO_2$ catalysts. Samples were reduced at 673 K prior to reaction.

reduction at 523, 673, and 773 K. Promotion causes a shift of selectivities from methane and acetaldehyde in Rh/573 to methanol and ethanol in Rh/X/573. The oxoselectivity, here defined as the sum of selectivities toward methanol, ethanol, and acetaldehyde, increases from 30% in Rh/573 to 79, 50, and 82% in V, Nb, and Ta oxide promoted Rh/573, respectively. The total oxoselectivities, S_{oxo}, are essentially independent of the temperature of reduction.

The influence of the temperature of calcination on the selectivities for methanol and ethanol is described in Fig. 5, for promoted Rh/SiO_2 catalysts after HT reduction. Except for $Rh/Nb/SiO_2$, where S_{EtOH} stays constant with calcination temperature, it is evident that S_{EtOH} decreases and S_{MeOH} increases for all catalysts when T_{calc} is raised from 573 to 1173 K. While this tendency is clear for $Rh/Ta/SiO_2$, it is less pronounced for $Rh/V/SiO_2$, where S_{MeOH} levels off at 973 K and S_{EtOH} seems to pass through a maximum.

DISCUSSION

Effect of Promotion

IR spectroscopy of adsorbed CO shows that all Rh/SiO_2 catalysts develop twin bands when heated from 85 K

to room temperature indicating that the metal dispersion must be sufficiently high to allow oxidative disruption of small Rh° clusters into $Rh^+(CO)_2$ cations. This process is described in Eq. [4] and reported previously (59, 60):

$$Rh^\circ + OH + 2CO \Rightarrow Rh^+(CO)_2 + 1/2H_2. \qquad [4]$$

Oxidation of Rh° to Rh^+ is effected by protons of hydroxyl groups. The metal dispersion is found to be high ($d < 3.5$ nm) for pure Rh/573 and all promoted Rh/573 catalysts. This has been proven by XRD for V, Nb, and Ta oxide promoted Rh/573 (51) and by TEM for V oxide promoted systems (47). It is noteworthy that the center of twin bands in all promoted Rh/X/573 catalysts is blue-shifted in the order Ta < Nb < V relative to Rh/573. The same is true for the stretching frequency of linearly bonded CO which is shifted to higher wavenumbers upon promotion of Rh/573 (see Table 1). This effect is more pronounced with decreasing atomic weight of the promoter element. The blue-shift of linearly bonded CO on Rh° metal clusters may be ascribed to a particle size effect as smaller particles exhibit a higher fraction of edge and corner atoms which are electron deficient (61). Additionally, the promoter oxide may electronically influence the CO stretching frequency of linearly bonded CO by polarization of small metal clusters (37). Weak bands which are detected in the region between 2150 and 2200 cm^{-1} (see Figs. 1, 2) can be ascribed to the interaction of CO with cus promoter cations. A close inspection of these bands was presented in a separate publication (51). Bands corresponding to CO stretching frequencies at 2197, 2192, and 2187 cm^{-1} which were recorded at low temperature after reduction at 673 K have been assigned to fourfold coordinated Ta^{5+}, Nb^{5+}, and V^{4+} sites, respectively.

Opposite shifts are observed for CO stretching frequencies of $Rh(CO)_2^+$ cations and of CO adsorbed on cus-promoter cations when the promoter element is varied. As apparent from Fig. 6, there is an almost linear correlation of ν_{CO} on cus sites of the promoter oxide with the center of twin bands ν_g, suggesting that the $Rh^+(CO)_2$ cations are electronically influenced by promoter oxide.

The rhodium dicarbonyl complex may be located directly on the promoter oxide or on silica oxygens which are electronically modified by adjacent promoter oxide. In the latter case, not only the carbonyl stretching frequency of the $Rh^+(CO)_2$ but also the O–H frequency of residual silanol groups should be affected. There is, however, no difference in the shift of the perturbed O–H stretching frequency of silanol groups upon LT adsorption of CO as evident from Fig. 3. It can be inferred that $Rh^+(CO)_2$ cations are located on the respective promoter oxides.

It is interesting that the presence of promoters also causes a change in the band shape of bridge-bonded CO on Rh°. A high frequency part at 1920 cm^{-1} which is present only

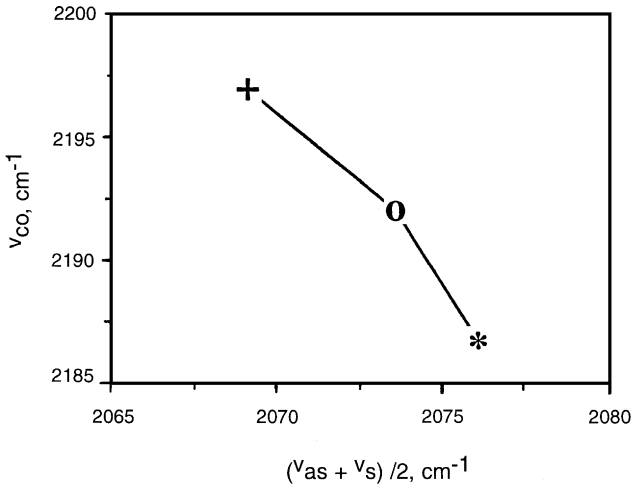

FIG. 6. Correlation of the ν_{CO} frequency of V^{4+}–CO (∗), Nb^{5+}–CO (○), and Ta^{5+}–CO (+) complexes measured in V/SiO_2, Nb/SiO_2 calcined at 573 K and Ta/SiO_2 calcined at 973 K, followed by reduction at 773 K, with the band center of twin bands in $Rh/V/SiO_2$ (∗), $Rh/Nb/SiO_2$ (○), and $Rh/Ta/SiO_2$ (+) calcined at 573 K and reduced at 673 K prior to CO adsorption.

in Rh/573 disappears in Rh/X/573. The band at 1920 cm^{-1} falls in the range of doubly bridging CO on Rh° and has been assigned to a $Rh_2(CO)_3$ structure with one bridging and two terminal CO ligands (62). The disappearance of this band in promoted Rh/573 catalysts suggests that these sites are modified by promoter oxide. This effect is, however, only observed after reduction to 673 or 773 K.

An evolution of the high frequency component of bridge-bonded CO on Rh° particles was observed earlier by Kraus *et al.* (33) when warming a Rh/SiO_2 catalyst from 80 to 300 K in CO. This effect was explained by activated morphological changes of the surface of big rhodium particles and was suppressed in the presence of niobium oxide. The effect described in this study is different in that it takes place at 80 and 300 K. The adsorption of CO at liquid N_2 temperature is considered a nondestructive method to probe surface sites which are originally present after reduction. The erosion of band intensity around 1920 cm^{-1} occurs already at 80 K when promoter oxides are present. The effect observed here can, therefore, not solely be ascribed to the inhibition of Rh° surface reconstructions by promoter oxides. Particle size effects, however, cannot be excluded.

Interestingly, the *l*/*b* ratio increases dramatically in HT reduced Rh/Nb/573 and Rh/Ta/573 catalysts. The *l*/*b* ratio is 4.3 in Rh/573, but increases to 6.8 and 7.1 in Rh/Nb/573 and Rh/Ta/573, respectively. A similar phenomenon has been observed for PdAg alloys in which linearly bonded CO on Pd° dominated over bridged-bonded CO with increasing Ag content (63). It is known that bridging CO

requires an ensemble of 2–4 atoms (64). The chemisorption results were explained with a dilution effect diminishing the size of surface Pd ensembles capable of adsorbing CO in a bridged fashion. On TiO_2 supported Ni films, Takatami and Chung (65) found an increased *l/b* ratio after reduction at 700 K by HREELS. It should be mentioned that the ratios of band intensities of linearly to bridge-bonded CO have been measured under reaction conditions by McQuire and Rochester (66) over unpromoted Rh/SiO_2. They found that this ratio remained constant even though changes in catalyst activity and selectivity occurred. They explained the spectral changes with the build up of carbonaceous deposits on the rhodium metal surface during catalysis. However, promoter oxide patches are chemically very different from coke deposits, and changes in the spectral feature of promoted Rh/SiO_2, as they were observed in this study, may well be a guideline to catalytic behavior.

Unpromoted Rh/573 yields mainly methane and acetaldehyde in agreement with literature data (8, 10). At given catalytic test conditions, the oxoselectivity of Rh/SiO_2 catalysts depends strongly on additives. Nonnemann *et al.* (67) showed recently that iron impurities present in the silica support enhance the ethanol selectivity. The very low ethanol selectivity measured over our Rh/SiO_2 catalyst is indicative of the absence of iron impurities. Promotion of Rh/SiO_2 leads to enhancement of the total activity and of the TOF in CO hydrogenation as evident from Tables 4 and 5. At the same time, oxoselectivity rises.

This effect was reported earlier and has been ascribed to the presence of metal promoter interfaces (14–18, 21–24). After LT reduction, the CO chemisorption capacities of samples Rh/Nb/573 and Rh/Ta/573 are enhanced compared to the unpromoted Rh/573 catalyst. This explains the increase in the total activity in the CO hydrogenation reaction as demonstrated in Fig. 4. The contact of Rh° with tetravalent Nb oxide and pentavalent Ta oxide, respectively, might be responsible for the shift in selectivities from acetaldehyde and methane in Rh/573 to oxoproducts methanol and ethanol in the promoted catalysts (see Tables 4 and 5). The shift of selectivities from acetaldehyde to ethanol points to an increase of the hydrogenation function of the catalyst. It is known that V_2O_3 can activate and store hydrogen (68). It was suggested that this might be crucial in order to obtain a sufficiently high H-concentration on the metal surface. The hydrogen coverage of the metal particles is decreased in the presence of coadsorbed CO (5). As this argument may well apply to V_2O_3 it is less likely to hold for NbO_2 and Ta_2O_5 whose reducibility is much lower. Assuming that ethanol is the hydrogenation product of acetaldehyde, one can imagine an acyl group as a common intermediate. The selectivity to either aldehyde or alcohol may then be explained in terms of a competitive hydrogenation of the C=O bond or M–C bond of the acyl group, respectively, as described in the reaction scheme:

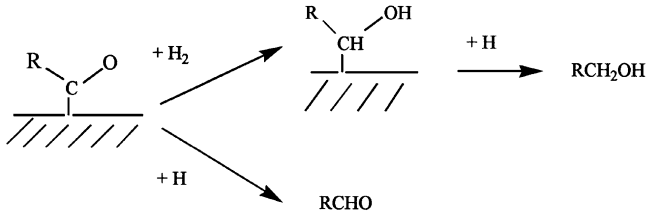

Influence of T_{red}

IR spectra of Rh/Nb/573 and Rh/Ta/573 (see Figs. 2A, B) after *LT reduction* look essentially identical to that of unpromoted Rh/SiO_2 (not shown). All systems exhibit a broad feature around 1920 cm^{-1}. It has been shown earlier (46) that the Rh° particle size does not change as a function of reduction temperature. The observed reduction of the absorbance at 1920 cm^{-1}, brought about in *HT reduced* and promoted Rh/573 catalysts, is most likely indicative of a partial coverage of Rh° particles by promoter oxide. This is in agreement with the decrease in CO chemisorption capacity reported in Ref. (51).

The jump in *l/b* ratios after HT reduction observed in this study can accordingly be rationalized by a decoration of the Rh° metal surface with promotor oxide patches such that the remaining ensembles are too small to accomodate bridging CO ligands. Hence, IR spectroscopy using CO as a probe proves to be a valuable tool in characterizing SMSI effects.

The reduction temperature has no influence on the total activity and selectivity of unpromoted Rh/SiO_2. This behavior is changed in promoted samples which exhibit a tendency of increasing ethanol selectivity with rising T_{red}. This trend is most pronounced in Rh/Ta/573. The production of ethanol seems to correlate with SMSI effects which have been induced by reduction. Interestingly, the total oxoselectivity remains essentially unaltered at different reduction temperatures for all promoted catalysts. There is a trend that HT reduced catalysts Rh/X/573 display higher TOFs compared to LT reduced ones.

Influence of T_{calc}

As was described separately, calcination to 973 or 1173 K leads to the formation of $RhXO_4$ mixed oxides (51). The reduction of Rh^{3+} ions in these oxides requires temperatures of 673 to 773 K and gives rise to well-dispersed Rh° particles which are included in a matrix of promoter oxide. CO chemisorption capacities for $Rh/X/SiO_2$ calcined to 973 K are very low except for $Rh/Ta/SiO_2$ for which sintering of Rh_2O_3 and formation of $RhTaO_4$ sets in only during calcination at 1173 K. In contrast, agglomeration of Rh_2O_3

occurs already at 973 K in unpromoted Rh/SiO_2. This is also evident from the integral intensities of adsorbed CO presented in Table 3. The *l/b* ratio after reduction at 673 K does not change much in Rh/SiO_2 regardless of the temperature of calcination, although the mean Rh° particle size increases dramatically from 3.5 nm in Rh/773 to 11 nm in Rh/1173, as was shown previously for similar Rh/SiO_2 catalysts prepared from a $RhCl_3$ precursor (46). In some cases increased *l/b* ratios have been observed with increasing metal dispersions (53, 69). Linearly bonded CO on Rh° metal particles should not be confused with the formation of linearly bonded CO on Rh^+ ions resulting from oxidative disruption of small Rh° metal clusters (see Eq. [4]). The relative population of linear and bridging CO ligands may also depend on the electron density at the Fermi level (70). As the *l/b* ratio is constant in Rh/SiO_2 there seems to be no significant change of the geometric or electronic properties of Rh° particles in an interval of mean sizes ranging from 3.5 to 11 nm.

The drop in *l/b* ratio from 7.3 in Rh/Ta/773 to 3.6 in Rh/Ta/1173 documents the appearance of large Rh° particles. Consequently, the total activity of Rh/Ta/1173 is substantially diminished and comparable to that of unpromoted Rh/573. Interestingly, Rh/V/1173 and Rh/Nb/1173 display roughly the same activity. In those systems, formation of mixed oxides $RhXO_4$ was established which transform into well-dispersed Rh° particles during HT reduction. No large Rh° particles were found in Rh/V/1173 and Rh/Nb/1173. Their low total activity in the CO hydrogenation thus suggests that small Rh° clusters are indeed entrapped in their respective matrix of promoter oxide. This was confirmed by the low CO chemisorption capacities of these catalysts (51). Obviously, these Rh° clusters are not, or only to a minor extent, liberated from their XO_y overlayer during catalysis indicating a strong metal-promoter oxide interaction. Remarkably, the selectivities for ethanol drop with rising temperature of calcination in all $Rh/X/SiO_2$ catalysts, whereas those for methanol grow. This effect is most pronounced for the $Rh/Ta/SiO_2$ system. Apparently, enhancement of metal promoter oxide interactions induced by calcination is unfavorable for the production of ethanol. S_{EtOH}, however, grows for Rh/Ta/573 with increasing temperature of reduction, that is, if the coverage of the Rh° metal is effected by reduction. The conventional, reduction induced SMSI effect tends to enhance ethanol formation rates, whereas the nonconventional, calcination induced SMSI effect favors formation of methanol.

Interestingly, TOFs increase in all promoted Rh/SiO_2 catalysts with rising temperature of calcination for all reduction temperatures, while overall activities decrease beyond $T_{calc} = 773$ K. This may be considered additional proof of a metal-promoter oxide interaction induced by air pretreatments.

CONCLUSIONS

Promotion of Rh/SiO_2 with Vb transition metal oxides leads to an increase in the overall CO hydrogenation activity. The promoting effect rises in the order V < Nb < Ta. Promotion enhances the selectivity for oxygenated products and provokes a shift in selectivities. While methane and acetaldehyde are main products over Rh/SiO_2, ethanol, and methanol are predominantly formed over promoted catalysts.

Two types of SMSI effects were studied, induced by HT reduction ($T_{red} \geq 673$ K) and HT calcination ($T_{calc} \geq 973$ K, followed by reduction at 673 K), respectively. SMSI effects which were induced by HT reduction caused an increase in ethanol selectivity, while those induced by HT calcination caused an increase in methanol selectivity.

The metal state was characterized using FTIR spectroscopy of adsorbed CO as a probe:

(1) Modification of Rh/SiO_2 with promoter oxide causes a slight blue-shift for linearly bonded CO on rhodium. $Rh(CO)_2^+$ cations which are detected in all catalysts are located on the silica support in Rh/SiO_2 but sit on the respective promoter oxides in $Rh/X/SiO_2$.

(2) Both reduction and calcination induced SMSI effects lead to a partial coverage of the rhodium metal surface by promoter oxide, the extent of which increases in the order Ta < Nb < V.

The SMSI state as induced by HT reduction gives rise to three characteristic changes in the spectral feature of catalysts as compared to reduction at low temperature ($T_{red} = 523$ K):

(1) The total CO chemisorption capacity is lowered.

(2) The relative amount of linearly to bridge-bonded CO increases, and

(3) characteristic changes in the band shape of bridge-bonded CO occur. A high frequency component of bridge-bonded CO at 1920 cm^{-1} which is present in the non-SMSI-state disappears after HT reduction.

ACKNOWLEDGMENTS

This work was financially supported by the Deutsche Forschungsgemeinschaft (SFB 338), the Bundesminister für Forschung und Technologie, and the Fonds der Chemischen Industrie; the studies were carried out in the framework of a joint research program sponsored by the Deutsche Forschungsgemeinschaft and the Russian Academy of Sciences. Gifts of niobic acid from CBMM and of tantalum oxalate solution from HCST are gratefully acknowledged.

REFERENCES

1. Kip, B. J., Hermans, E. G. F., van Wolput, J. H. M. C., Hermans, N. M. A., van Grondelle, J., and Prins, R., *Appl. Catal.* **35**, 139 (1987).
2. Bhasin, M. M., Bartley, W. T., Ellgen, P. C., and Wilson, T. P., *J. Catal.* **54**, 120 (1978).

3. Kawai, M., Uda, M., and Ichikawa, M., *J. Phys. Chem.* **89**, 1654 (1985).
4. Lisitsin, A. S., Stevenson, S. A., and Knözinger, H., *J. Mol. Catal.* **63**, 201 (1990).
5. Van den Berg, F. G. A., Glezer, J. H. E., and Sachtler, W. M. H., *J. Catal.* **93**, 340 (1985).
6. Ehwald, H., Ewald, H., Gutschick, D., Hermann, M., Miessner, H., and E. Schierhorn, E., *Appl. Catal.* **76**, 153 (1991).
7. Inoue, M., Nakajima, K., Kurusu, A., Miyake, T., and Inui, T., *Appl. Catal.* **49**, 217 (1989).
8. Orita, H., Naito, S., and Tamaru, K., *J. Catal.* **90**, 183 (1984).
9. Hindermann, J. P., Kiennemann, A., and Taarit, B., *Stud. Surf. Sci. Catal.* **48**, 481 (1989).
10. Underwood, R. P., and Bell, A. T., *Appl. Catal.* **21**, 157 (1986).
11. Burch, R., and Petch, M. I., *Appl. Catal.* **88**, 39 (1992).
12. Kuznetzov, V. L., Romanenko, A. V., Mudrakowskii, I. L., Mastikhin, V. M., Shmachkov, V. A., and Yermakov, Yu. I., *in* "Proceedings 8th Int. Congr. Catal., Berlin 1984," Vol. 3, Verlag Chemie, Weinheim, 1984.
13. Ponec, V., *Catal. Today* **12**, 227 (1992).
14. Kip, B. J., Hermans, E. G. F., and Prins, R., *Appl. Catal.* **35**, 141 (1987).
15. Van der Lee, G., Schuller, L., Post, H., Favre, T. L. F., and Ponec, V., *J. Catal.* **98**, 522 (1986).
16. Van der Lee, G., Bastein, A. G. T. M., van den Boogert, J., Schuller, B., Luo, H., and Ponec, V., *J. Chem. Soc. Faraday Trans. 1* **83**, 2103 (1987).
17. Bastein, A. G. T. M., van den Boogert, W. J., van der Lee, G., Luo, H., Schuller, B., and Ponec, V., *Appl. Catal.* **29**, 243 (1987).
18. Kowalski, J., van der Lee, G., and Ponec, V., *Appl. Catal.* **19**, 423 (1985).
19. Kip, B. J., Smeets, P. A. T., van Grondelle, J., and Prins, R., *Appl. Catal.* **33**, 181 (1987).
20. Van der Lee, G., and Ponec, V., *Catal. Rev.-Sci. Eng.* **29**, 183 (1987).
21. Koerts, T., Welters, W. J. J., and van Santen, R. A., *J. Catal.* **134**, 1 (1992).
22. Koerts, T., and van Santen, R. A., *J. Catal.* **134**, 13 (1992).
23. Luo, H., Zhou, H., Lin, L., Liang, D., Li, C., Fu, D., and Xin, Q., *J. Catal.* **145**, 232 (1994).
24. Mori, T., *Catal. Lett.* **7**, 151 (1990).
25. Johnston, P., Joyner, R. W., Pundney, P. D. A., Shpiro, E. S., and Williams, B. P., *Faraday Disc. Chem. Soc.* **89**, 91 (1990).
26. Wang, R., and Xu, Y., *J. Mol. Catal.* **54**(3), 478 (1989).
27. Il'chenko, N. I., Shmyrko, Yu. I., Raevskaya, L. N., and Golodets, G. I., *Teor. Eksp. Khim.* **24**(5), 612 (1988).
28. Luo, H. Y., Bastein, A. G. T. M., Mulder, A. A. J. P., and Ponec, V., *Appl. Catal.* **38**, 241 (1988).
29. Kunimori, K., Hu, Z., Uchijima, T., Asakura, K., Iwasawa, Y., and Soma, M., *Catal. Today* **8**, 85 (1990).
30. Sachtler, W. M. H., and Ichikawa, M., *J. Phys. Chem.* **90**, 4752 (1986).
31. Kunimori, K., Abe, H., and Uchijima, T., *Chem. Lett.* 1619 (1983).
32. Alekseev, O. A., Beutel, T., Paukshtis, E. A., Ryndin, Yu. A., and Knözinger, H., *J. Mol. Catal.* **92**, 217 (1994).
33. Kraus, L., Zaki, M. I., Knözinger, H., and Tesche, B., *J. Mol. Catal.* **55**, 55 (1989).
34. Akubuiro, E. C., Ionnides, T., and Verykios, X. E., *J. Catal.* **116**, 590 (1989).
35. Tauster, S. J., and Fung, S. C., *J. Catal.* **55**, 29 (1978).
36. Brewer, L., *Science* **161**, 115 (1968).
37. Van Santen, R. A., *in* "Fundamental Aspects of Heterogeneous Catalysis Studied by Particle Beams" (H. H. Brongersma and R. A. van Santen, Eds.), p. 83, Plenum, New York, 1991.
38. Horsley, J. A., *J. Am. Chem. Soc.* **101**, 2870 (1979).
39. Meriaudeau, P., Dutel, J. F., Dufaux, M., and Naccache, C., *Stud. Surf. Sci. Catal.* **11**, 95 (1982).
40. Resasco, D. E., and Haller, G. L., *J. Catal.* **82**, 279 (1983).
41. Chen, B.-H., and White, J. M., *J. Phys. Chem.* **87**, 1327 (1983).
42. Taglauer, E., and Knözinger, H., *Phys. Stat. Sol. (b)* **192**, 465 (1995).
43. Boffa, A. B., Bell, A. T., and Somorjai, G. A., *J. Catal.* **139**, 602 (1993).
44. Hu, Z., Wakasugi, T., Maeda, A., Kunimori, K., and Uchijima, T., *J. Catal.* **127**, 276 (1991).
45. Kunimori, K., Shindo, H., Oyanagi, H., and Uchijima, T., *Catal. Today* **16**, 387 (1990).
46. Beutel, T., Knözinger, H., Siborov, A. V., and Zaikovskii, V. I., *J. Chem. Soc., Faraday Trans.* **88**, 2775 (1992).
47. Tesche, B., Beutel, T., and Knözinger, *J. Catal.* **149**, 100 (1994).
48. Hu, Z., Nakamura, K., Kunimori, K., Yokoyama, Y., Asano, H., Soma, M., and Uchijima, T., *J. Catal.* **119**, 33 (1989).
49. Yin, Y. G., Wakasugi, T., Shindo, H., Ito, S., Kunimori, K., and Uchijima, T., *Catal. Lett.* **9**, 43 (1991).
50. Kunzmann, G., Dissertation, Univ. of Munich, 1987 (unpublished).
51. Beutel, T., Siborov, A. V., Tesche, B., and Knözinger, H., *J. Catal.*, to appear.
52. Deleted in proof.
53. Yang, A. C., and Garland, C. W., *J. Phys. Chem.* **61**, 1504 (1957).
54. Van't Blik, H. F. J., van Zon, J. B. A. D., Huizinga, T., Vis, J. C., Koningsberger, D. C., and Prins, R., *J. Am. Chem. Soc.* **107**, 3139 (1985).
55. Basu, P., Panayotov, D., and Yates, J. T., Jr., *J. Phys. Chem.* **90**, 5312 (1987).
56. Worley, S. D., Rice, C. A., Mattson, G. A., Curtis, C. W., Guin, J. A., and Tarrer, A. R., *J. Phys. Chem.* **86**, 2714 (1982).
57. Rasband, P. B., Hecker, W. C., *J. Catal.* **139**, 551 (1993).
58. Yoshitake, H., Asakura, K., and Iwasawa, Y., *J. Chem. Soc., Faraday Trans. 1* **84**, 4337 (1988).
59. Smith, A. K., Hugues, F., Theolier, A., Basset, J. M., Ugo, R., Zanderighi, G. M., Bilhou, J. L., Bilhou-Bougnol, V., and Grayon, W. F., *Inorg. Chem.* **18**, 3104 (1979).
60. Wong, T. T. T., Stakheev, A. Yu., and Sachtler, W. M. H., *J. Phys. Chem.* **96**, 7740 (1992).
61. Estiu, G. L., and Zerner, M. C., *J. Phys. Chem.* **97**, 13720 (1993).
62. Rice, C. A., Worley, S. D., Curtis, C. W., Guin, J. A., and Tarrer, A. R., *J. Chem. Phys.* **74**, 6487 (1981).
63. Primet, M., Mathieu, M. V., and Sachtler, W. M. H., *J. Catal.* **44**, 324 (1976).
64. Sheppard, N., Ngyuen, T. T., "Advances in Infrared and Raman Spectroscopy," Vol. 5, pp. 67–86, Heyden, 1978.
65. Takatami, S., and Chung, Y. W., *J. Catal.* **90**, 75 (1984).
66. McQuire, M. W., and Rochester, C. H., *Ber. Bunsenges. Phys. Chem.* **97**, 298 (1993).
67. Nonnemann, L. E. Y., Bastein, A. G. T. M., and Ponec, V., *Appl. Catal.* **62**, L23 (1990).
68. Bond, G. C., Shermon, P. A., and Wright, C., *J. Mater. Res. Bull.* **19**, 701 (1984).
69. Wanke, S. E., and Dougharty, N. A., *J. Catal.* **24**, 3 (1972).
70. Van Santen, R. A., *J. Chem. Soc., Faraday Trans. 1* **83**, 1915 (1987).